# Non-stationary Coulomb crystals in linear Paul traps



2003 J. Phys. B: At. Mol. Opt. Phys. 36 525

(http://iopscience.iop.org/0953-4075/36/3/310)

INSTITUTE OF PHYSICS PUBLISHING JOURNAL OF PHYSICS B: ATOMIC, MOLECULAR AND OPTICAL PHYSICS

J. Phys. B: At. Mol. Opt. Phys. **36** (2003) 525–532 PII: S0953-4075(03)54386-3

# Non-stationary Coulomb crystals in linear Paul traps

**Michael Drewsen[1], Inger S Jensen, Niels Kjærgaard, Jens Lindballe, Anders Mortensen, Kristian Mølhave and Dirk Voigt**

Department of Physics and Astronomy, University of Aarhus, Ny Munkegade, Bld. 520, DK-8000 Aarhus C, Denmark

E-mail: drewsen@phys.au.dk

Received 23 September 2002, in final form 22 November 2002
Published 23 January 2003
Online at stacks.iop.org/JPhysB/36/525

**Abstract**

Ion Coulomb crystals form when trapped ions are cooled below a certain critical temperature. In radiofrequency (RF) traps, such crystals are usually stationary (i.e. non-rotating) with shapes similar to those of cold, homogeneously charged liquids when the number of ions is sufficient for three-dimensional structures to appear. 'Dynamically stable' structures can, however, also be created either by directly applying a torque to an initially stationary crystal or by choosing trap parameters just within the stability region where stationary crystals will melt due to parametric resonances between the RF trap field and ion plasma modes.

## 1. Introduction

When trapped ions are cooled below a certain critical temperature (typically about 10 mK) they form spatially ordered structures, often referred to as ion Coulomb crystals. In the last decade, such crystals of various sizes containing single-ion species have been investigated in various types of traps (see, e.g. [1–6] and references therein). In a number of recent experiments, the detailed structures of such crystals have been shown to be in good agreement with theoretical predictions [1–6] and the shape of the outer boundary of these cold plasmas has been shown to be very similar to that of a cold, homogeneously charged liquid [7] for a large variety of trapping parameters (see [8, 9]). As an example, CCD images of an ion Coulomb crystal consisting of about 100 ions are shown for five different potentials of a linear Paul trap in figure 1. As is evident from figure 2, only in the extreme limits where the ion Coulomb crystal becomes one-dimensional string-like or two-dimensional pancake-like do deviations from the liquid model appear. The latter is clearly seen in figure 2, when the aspect ratio of the crystal is above 20. Whereas ion Coulomb crystals in Penning traps are forced to rotate in order to be confined, in radiofrequency (RF) traps ion crystals are normally non-rotating as in the crystals shown in figure 1. In this paper we will present some preliminary results showing that in

[1] Author to whom any correspondence should be addressed.

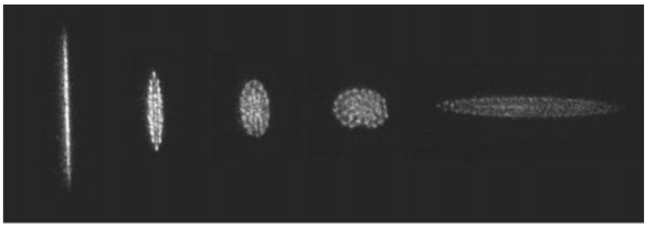

**Figure 1.** CCD images of an ion Coulomb crystal of about 100 $^{24}Mg^{+}$ ions for five different trapping potentials. The crystals are rotationally symmetric around the left–right axis of the figure. The first image corresponds to a nearly pancake-like structure while the last one is cigar-shaped. The radial trap frequency $\omega_r$ is given by $\omega_r = (\omega_\rho{}^2 - 0.5\omega_z{}^2)^{1/2}$, where $\omega_\rho = 2\pi \times 300$ kHz and $\omega_z$ is the axial trap frequency. In units of $\omega_\rho$, the value of $\omega_z$ is 1.37, 1.31, 1.01, 0.56 and 0.235, respectively, for the five crystals presented.

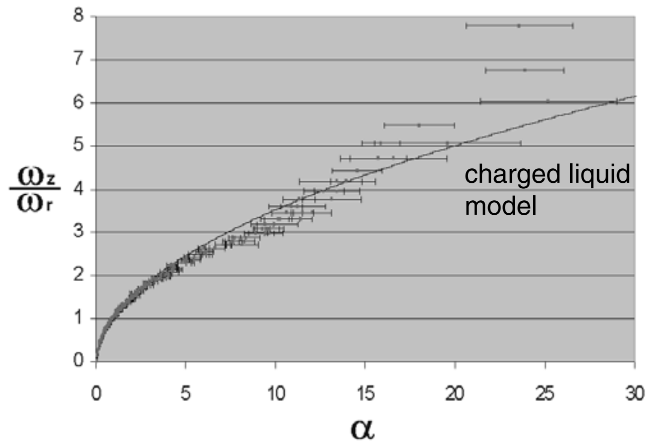


**Figure 2.** Measured radial to axial aspect ratio $\alpha$ of the crystal shown in figure 1 for corresponding calculated ratio of the axial to radial trap oscillation frequencies, $\omega_z/\omega_r$. The two graphs show the expected relation between these two quantities in a non-interacting particle and a cold homogeneously charged liquid model.

linear Paul traps rotating crystals can be created by exerting a torque on an initially stationary crystal. We will also show that 'dynamically stable' crystals can be formed by choosing trap parameters just within the stability region where stationary crystals will melt due to parametric resonances between the RF trap field and ion plasma modes.

## 2. Laser-torque-induced rotating crystals

While for many years the torque produced by the radiation pressure force of a near-resonant laser beam intersecting a cold ion plasma off-axis has been applied to control the plasma rotation frequency in Penning traps [10], the same technique has not, to our knowledge, previously been tested on cold ion ensembles in RF traps. In the preliminary experiments we have performed, first a non-rotating ion crystal was formed by laser cooling $^{40}Ca^{+}$ ions along the RF field free axis of a linear Paul trap (details on the trap used can be found in [11]). An example of such a non-rotating crystal consisting of $\sim$200 ions is shown in figure 3(a). Next, a 'torque' beam with a power $\sim$1 mW derived from the same laser as the cooling beams is focused to a spot size of about 100 $\mu$m where it crosses the ion crystal in a direction perpendicular to the cooling beams. By either changing the offset position of the torque beam with respect to the central RF field free axis, detuning the laser or the laser power, stable rotating crystals with significantly changed crystal aspect ratios could be formed. In figures 3(b)–(f) a series of such rotating crystals obtained by only changing the offset position of the 'torque' laser are shown (the corresponding stationary crystal is the one shown in figure 3(a)). In the case of figure 3(f), the rotating crystal is extremely oblate, indicating that the rotation frequency is close to the radial trap frequency, which is $\omega_r = 2\pi \times 180$ kHz. The structures of the rotating crystals seem to be more or less identical to stationary crystals with equivalent aspect ratios (see figure 1). Besides the shape and structures, the hypothesis of rotation in the case of figures 3(b)–(f) is supported by the fact that the ion density scales (within the uncertainty of the measurements) as $(\omega_{r,eff}/\omega_z)^2+1/2$ (expected from theory), where $\omega_{r,eff}$ is the effective radial trap frequency, including the centrifugal force due to rotation, and $\omega_z$ is the axial trap frequency (independent of the rotation frequency). The values of $\omega_{r,eff}/\omega_z$ have been deduced from the aspect ratios of the crystals through the relation given by the solid curve in figure 2.

Besides being fascinating objects, rotating crystals might also prove to be very useful in quantifying sympathetic cooling of the radial degrees of freedom of an ion plasma when applying laser cooling only along the RF field free axis. (This is usually the situation when producing larger crystal structures in linear Paul traps [2, 12].) If after a crystal has reached a steady rotational state the laser beam providing the torque is turned off, one can monitor, as function of time, how fast the crystal relaxes towards the non-rotating stationary state and hence deduce an effective radial cooling rate. In figure 4, a series of CCD images of a cold ion plasma is presented for different times after shutting off the torque-producing laser beam (the time interval between the pictures is 166 ms). From the known trap potential and the aspect ratio of the individual cold plasmas presented in figure 4, one can determine the total rotational energy of the ion cloud through the relation to the effective axial and radial confining potential (solid curve figure 2) for each picture. In figure 5, this rotational energy per ion is plotted as a function of time after blocking the torque laser together with an exponential fit from which a typical cooling timescale of $\sim$100 ms can be derived. This timescale is considerably longer than the typical optimum Doppler laser cooling time of $\sim$100 $\mu$s. Though it is not exactly correct to compare the found radial cooling time constant with the time constant for three-dimensional sympathetic cooling of one ion species by another laser-cooled species, the values are definitely linked and apparently very similar. From further detailed studies of sympathetic radial cooling of rotating crystals one might be able to provide new experimental insight into three-dimensional sympathetic cooling. Sympathetic radial cooling must also play a crucial role for the steady rotation frequency of ion crystals such as those presented in figure 3. While the force from the torque-laser beam alone would lead to an ever increasing rotational frequency, the presence of the rotational damping force induced by the cooling lasers could provide the needed friction in the system to obtain a well-defined locking frequency.

In the experiments, any torque provided by slight misalignment of the cooling laser beams was too insignificant to lead to crystal rotation.

## 3. Parametric-resonance-induced 'dynamically stable' crystals

Another type of 'dynamically stable' crystal structure is apparently linked to parametric resonances between the frequency of the radial confining trap field and plasma modes of the ion crystals. These structures are easily observed when operating the linear Paul trap by a periodic sequence of square pulses, as sketched in figure 6 (see also [11]). In figure 4, the single-ion stability diagram is shown with an indication of the region where stationary $^{24}Mg^+$ ion Coulomb

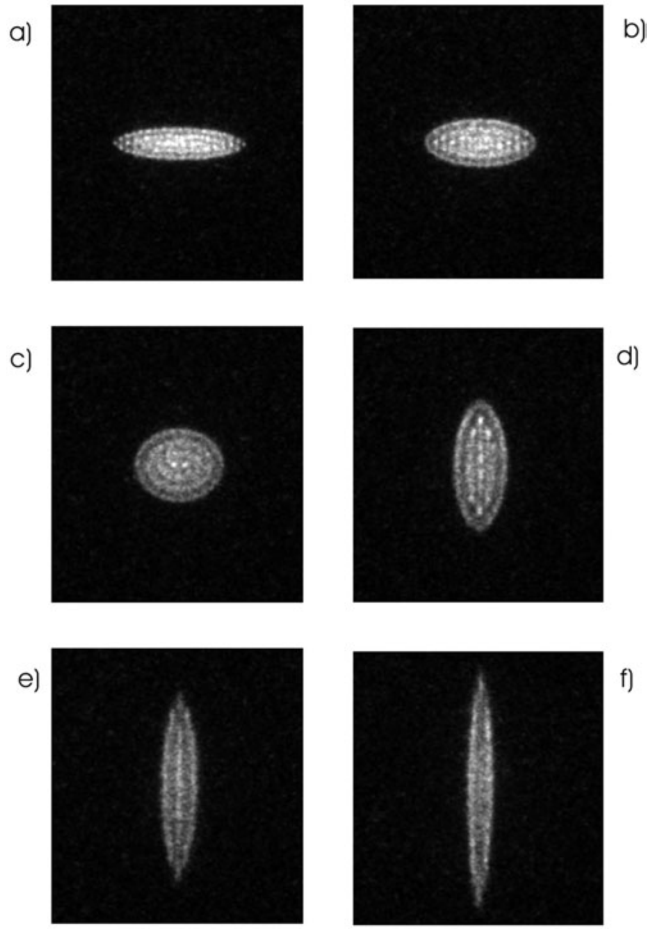


**Figure 3.** Pictures of an ion crystal consisting of ∼200 ions at various rotation frequencies induced by the torque of a laser beam. The symmetry axis along which laser cooling is provided is left–right in the figures. The crystal in (a) is stationary, while the other pictures represent increasing rotational frequency with the rotational frequency being: (b) $0.4\omega_{r,trap}$, (c) $0.7\omega_{r,trap}$, (d) $0.9\omega_{r,trap}$, (e) $0.96\omega_{r,trap}$ and (f) $0.98\omega_{r,trap}$, where $\omega_{r,trap} = 2\pi \times 180$ kHz is the radial trap frequency. For reference, the axial trap frequency was in all the experiments $\omega_z = 2\pi \times 86$ kHz. The width of each picture corresponds to a real length of 800 $\mu$m.

crystals have been observed. The vertical line in this figure represents a rough theoretical limit for stable crystals due to the appearance of parametric resonances between the RF frequency $\omega_{RF}$ of the trapping field and a mode frequency $\omega_{mode}$ of the crystals. Formally, this parametric resonance condition reads: $2\omega_{RF} = \omega_{mode}$. For larger crystals the mode frequencies cover a broad range with the maximal frequency $\omega_{mode,max}$ being close to the plasma frequency $\omega_{plasma}$ of an infinite crystal [13]. More precisely, the vertical line actually defines the trap parameters where $2\omega_{RF} = \omega_{plasma}$. To the right of the line $2\omega_{RF} < \omega_{plasma}$, which means that parametric resonances will be present for larger crystals. As is evident from figure 7, stationary crystals are accordingly not observed to the right of the stability line. At trap parameters where parametric resonances will lead to melting of stationary crystals, rotating crystals, which have lower densities, might exist since $\omega_{plasma}$ scales as the root of the ion density. In a series of

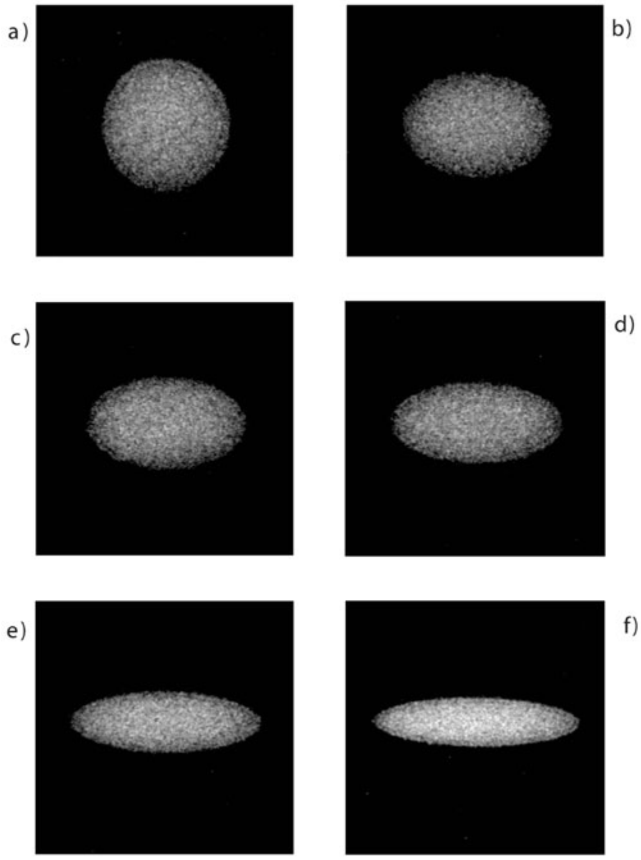


**Figure 4.** Pictures showing the rotational relaxation of a cold ion plasma containing a few thousand ions after the laser beam used to spin-up the cold cloud has been blocked. The time interval between the images is 166 ms. The width of each picture corresponds to a real length of 1.1 mm.

experiments, we have first created ion crystals within the stability region of stationary crystals (horizontally hatched area in figure 7) and then increased the amplitude of the square pulses applied to the trap (equivalent to increasing the value of the stability parameter $q$) until the stability line was just passed. Immediately before crossing the line, normal stationary crystals like the one shown in figure 8(a) were observed, while when passing the line, the crystal first melted, but within seconds reordered to form a completely different 'dynamically stable' structure as shown in figure 8(b). These structures are extremely axially ordered with an outer spheroidal contour like the stationary and rotating crystals discussed in the previous sections. The outer shape of the crystal in figure 8(b) can actually be explained if the ions in the ordered structure are rotating at a frequency equal to $\sim 0.3\omega_{RF}$. This hypothesis is supported by a series of experiments where the aspect ratios of the ordered structures were measured for various axial trap frequencies. An excellent agreement with the cold liquid model shown in figure 2 was found when a rotation frequency of $0.3\omega_{RF}$ was included in the calculation of the effective radial confining potential. Though locking to a specific rotational frequency can be understood as a balance between the sympathetic radial cooling (see the previous section) by the direct axial laser cooling and heating from parametric resonances, the value of the rotation frequency as well as the axial ordering remains to be understood. Finally, the mechanism triggering the

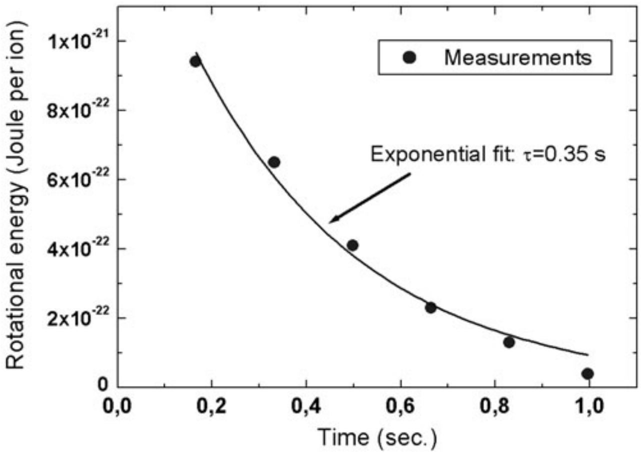


**Figure 5.** Plot of the rotational energy per ion as a function of time after blocking the torque laser together with an exponential fit which determines an effective radial cooling time.

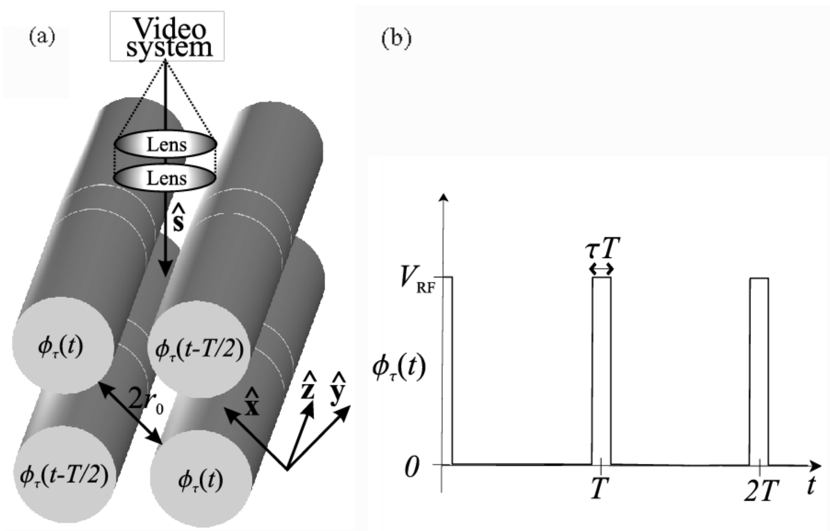


**Figure 6.** Sketch of the linear Paul trap showing the time-varying potentials applied to the electrodes. (b) Sketch of the time-varying potential $\phi_\tau(t)$ applied to the trap. $T$ represents the period of the square pulse potential, while $\tau$ defines the relative length of the pulses.

rotation has still not been determined, but a weak torque on the ion plasma due to a slight misalignment of the cooling laser beam with respect to the RF free trap axis could be the explanation.

The observed 'dynamically stable' structures might well be interesting in connection with crystallization experiments in storage rings where the radial confinement is equivalent to that of a pulse-operated linear Paul trap [11].

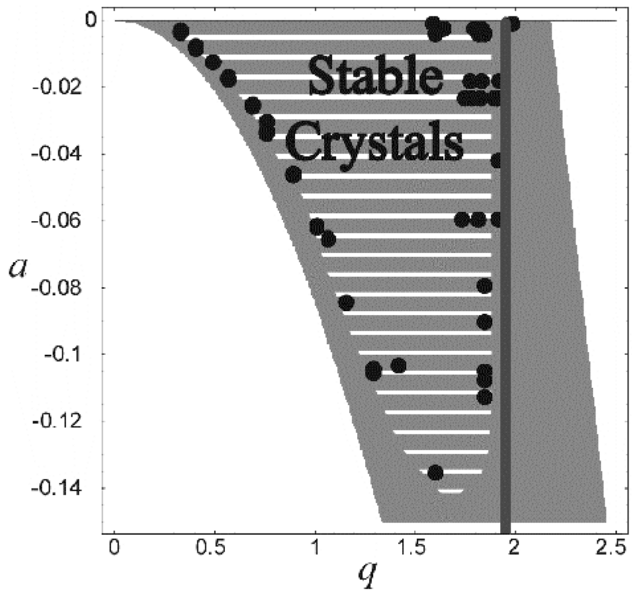


**Figure 7.** Single-ion stability diagram (grey-shaded area) including the area where larger stationary Coulomb crystals have been observed (horizontally hatched area) and a line indicating a rough theoretical limit for stable stationary crystals due to parametric resonances (crystals are stable to the left of the line). The dots indicate experiments where crystals were observed to be unstable. The stability parameters $a$ and $q$ are defined as follows: $q = 2eV_{RF}/mr_0^2\omega_{RF}^2$ and $a = 4\eta eU_{DC}/mr_0^2\omega_{RF}^2$, where $e$ and $m$ are the charge and the mass of the ion, $V_{RF}$ is the amplitude of the time-varying pulses applied to the trap as pointed out in figure 6, $\omega_{RF} = 2\pi/T$, with $T$ being the pulse period, $U_{DC}$ is the continuous dc voltage applied to the eight end-pieces of the electrodes shown in figure 6 for axial confinement and $\eta = 0.99$ is a parameter determined by the geometry of the trap. Furthermore, $\tau = 0.1$ has been used in calculating the stability diagram.

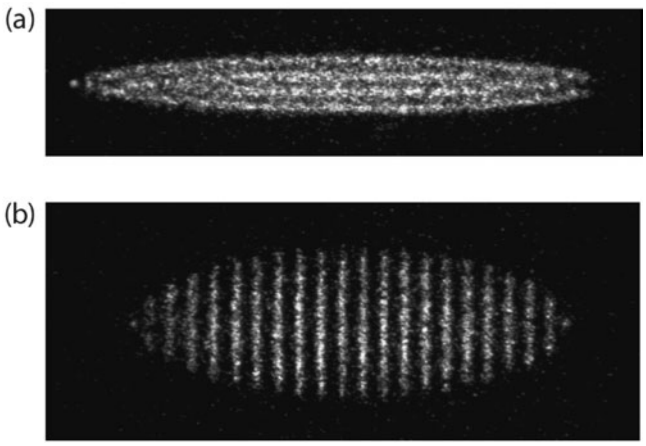


**Figure 8.** Two examples of ion crystals observed for $T = 10^{-6}$ s and $\tau = 0.1$ and $a > -0.02$ just to the left (a) and just to the right (b) of the line in figure 7 representing the theoretical prediction of parametric resonance. Note the very different shapes and ordering of these two crystals.

## 4. Conclusion

It has been shown that non-stationary ion Coulomb crystals can be formed in linear Paul traps either by applying a torque induced by a near-resonant laser beam or through a parametric coupling of the ion plasma to the RF field applied to the trap electrodes. The crystal structures in the first case resemble those of stationary crystals, while in the latter case unusual strong axial ordering exists.

## Acknowledgments

This work is supported by the Danish National Research Foundation, through QUANTOP-Danish National Research Foundation Centre for Quantum Optics, and the Carlsberg Foundation.

## References

[1] Birkl G, Kassner S and Walther H 1992 *Nature* **357** 310
[2] Drewsen M *et al* 1998 *Phys. Rev. Lett.* **81** 2878
[3] Itano W M *et al* 1998 *Science* **279** 686
[4] Mitchell T B *et al* 1999 *Science* **282** 1290
[5] Block M, Drakoudis A, Leutner H, Siebert P and Werth G 2000 *J. Phys. B: At. Mol. Opt. Phys.* **33** L375
[6] Schätz T, Schramm U and Habs D 2001 *Nature* **412** 717
[7] Turner L 1987 *Phys. Fluids* **30** 3196
[8] Brewer L R *et al* 1988 *Phys. Rev.* A **38** 859
[9] Drewsen M *et al* 2002 *Proc. Non-Neutral Plasma Physics IV (San Diego, CA, 2002) (AIP Conf. Proc. vol 606)* (New York: American Institute of Physics) p 135
[10] Bollinger J J and Wineland D J 1984 *Phys. Rev. Lett.* **53** 348
[11] Kjærgaard N, Mølhave K and Drewsen M 2002 *Phys. Rev.* E **66** 015401(R)
[12] Hornekær L *et al* 1994 *Phys. Rev. Lett.* **86**
[13] Dubin D H E and Schiffer J P 1996 *Phys. Rev.* E **53** 5249